ELSEVIER

Thermochimica Acta 352–353 (2000) 265–271

thermochimica acta

www.elsevier.com/locate/tca

Heat capacity of $(Hf_{1-y}Al_y)O_{0.17}$ at high temperature

Toshihide Tsuji[a,*], Tetsuya Kato[b]

[a]*Center for New Materials, Japan Advanced Institute of Science and Technology, Hokuriku, 1-1 Asahidai, Tatsunokuchi, Ishikawa 923-1292, Japan*

[b]*Physical Chemistry Department, Central Research Institute of Electric Power Industry, Iwadokita 2-Chome 11-1, Komae, Tokyo 201-0004, Japan*

Received 2 June 1999; received in revised form 30 August 1999; accepted 7 September 1999

Abstract

Heat capacities of $(Hf_{1-y}Al_y)O_{0.17}$ (y=0–0.03) were measured from 325 to 905 K by using an adiabatic scanning calorimeter. A heat capacity anomaly was observed around 700 K for all $(Hf_{1-y}Al_y)O_{0.17}$ samples and assigned to an order–disorder rearrangement of oxygen atoms. The experimental transition temperatures, the enthalpy change and entropy changes due to the order–disorder transition decreased with increasing aluminium contents. The experimental entropy changes of the order–disorder transition are compared with the theoretical values from the view point of statistical thermodynamics and are discussed.

Keywords: Heat capacity; Hafnium oxide; Order–disorder transition; Heat capacity anomaly; Transition entropy

1. Introduction

It is known that the α phase of IVA transition metals namely, titanium, zirconium and hafnium, dissolves up to 29 at.% (O/Ti=x=0.41) [1], 30 at.% (O/Zr=x=0.43) [2] and 20 at.% (O/Hf=x=0.25) [3,4] of oxygen, respectively, in the octahedral holes of the hcp metal sublattice. The dissolved oxygen atoms form ordered structures at higher oxygen-to-metal ratios and at low temperatures [5]. In our laboratory, heat capacities of titanium– [6], zirconium– [7] and hafnium–oxygen [8,9] solid solutions were measured in order to clarify the order–disorder behavior of the oxygen atoms and the results were discussed using statistical thermodynamics models of order–disorder changes [5].

For hafnium–oxygen solid solutions, Hirabayashi et al. [10] determined the ordered structure of HfO_x by electron and neutron diffraction methods. Two ordered crystal structures of oxygen sublattices for (a) $HfO_{(1/6)(-)}$ and (b) $HfO_{(1/6)(+)}$ are shown in Fig. 1. The basic ordered structure was the ordered one for x=1/6. Oxygen vacancies exist for x<1/6 and interstitial oxygen atoms for x>1/6 in the basic ordered structure. We measured the heat capacities of HfO_x (x=0.11–0.22) from 325 to 905 K by using an adiabatic scanning calorimeter [8,9]. A heat capacity anomaly was observed for all samples around 700 K and assigned to order–disorder transition of oxygen sublattice. The experimental transition entropy changes obtained in our previous study were larger than those reported by Hirabayashi et al. [10]. It was also found that the experimental transition entropy change for the composition of x=0.17 (x∼1/6) in our previous study was in good agreement with the theoretical transition

* Corresponding author. Fax: +81-761-51-1455.
E-mail address: tsuji@jaist.ac.jp (T. Tsuji)

0040-6031/00/$ – see front matter
PII: S0040-6031(99)00475-X

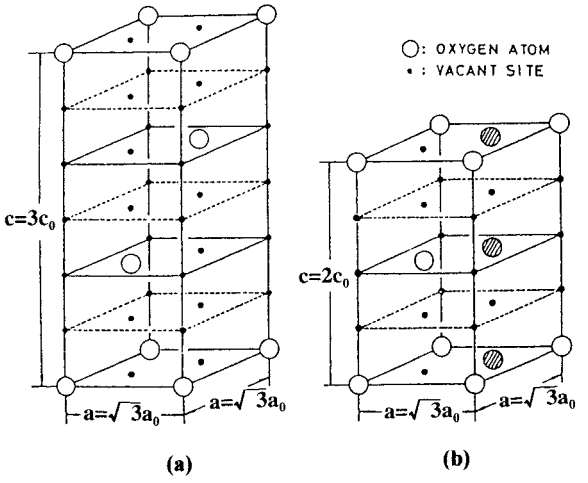

Fig. 1. Two ordered oxygen sublattices of (a) $HfO_{(1/6)(-)}$ and (b) $HfO_{(1/6)(+)}$. (○) oxygen atoms. (●) vacant octahedral sites. (▨) Next inserted oxygen interstitial sites.

entropy change calculated using statistical thermodynamics. On the other hand, the experimental values for the other compositions ($x \neq 0.17$) were smaller than the theoretical values. This difference was attributed to the increasing degree of freedom for configuration in the ordered structures due to the increments of oxygen vacancies for $x<1/6$ or the increments of interstitial oxygen atoms for $x>1/6$.

In this paper, we describe the results of heat capacity measurements of $(Hf_{1-y}Al_y)O_{0.17}$ from 325 to 905 K aiming to know the effect of doped metals on the order–disorder phase transition. The experimental entropy changes of the order–disorder transition obtained are compared with the theoretical values from a statistical thermodynamics model of order–disorder.

2. Experimental

2.1. Sample preparation and characterization

Hafnium metal sponge was oxidized for 3 h at 773 K in air and the amounts of oxygen in the oxidized hafnium were determined from the weight gain of the hafnium metal. The oxidized hafnium metal, hafnium metal sponge and aluminium powders were mixed in appropriate ratios and melted a few times under an argon gas stream in a plasma jet furnace. The ingot sample thus obtained was sealed in an evacuated silica tube, annealed for 3 days at 1273 K to homogenize the oxygen dissolved in the sample and cooled to room temperature. The homogenized ingot was crushed into pieces of less than 3–5 mm in size by using a stainless-steel mortar. The crushed sample of about 36 g was sealed in a quartz vessel with a helium gas pressure of 20 kPa to ensure high thermal conductivity in the vessel during heat capacity measurements. The sealed sample was then annealed between 603 and 623 K for 2 weeks to form the ordered structures and cooled slowly in 1 week to ambient temperature. The homogenized samples were characterized using the X-ray diffraction method. The O/(Hf+Al) ratio of each sample was determined from weight gain in oxidation to (Hf, Al)O_2. The determined compositions were in good agreement with the initial compositions.

2.2. Heat capacity measurement

Heat capacity measurements of $(Hf_{1-y}Al_y)O_{0.17}$ (y=0–0.03) were carried out using an adiabatic scanning calorimeter from 325 to 905 K as described elsewhere [8,9]. The scanning heating rate chosen in this study was 2 K min^{-1} under a pressure of about 2 kPa of air in the calorimeter. Heat capacity measurements using the calorimeter were standardized by measurements on pure zirconium metal. In comparison with the data of Douglass [11], the imprecision and the inaccuracy were determined to be +5% and ±3%, respectively.

We carried out heat capacity measurements in the following procedure to obtain the experimental transition entropy changes. The first series of measurements was carried out on the samples before annealing. These heat capacity data were used for determinations of the baselines required to estimate the experimental transition entropy changes as described later. The samples were then annealed at temperatures between 603 and 623 K for 2 weeks to form the ordered structures in the interstitial oxygen sublattice and cooled slowly in 1 week to ambient temperature. The second series of measurements was carried out on these well-annealed samples, and the experimental transition enthalpy and entropy changes were determined from the excess heat capacity of the order–disorder transition.

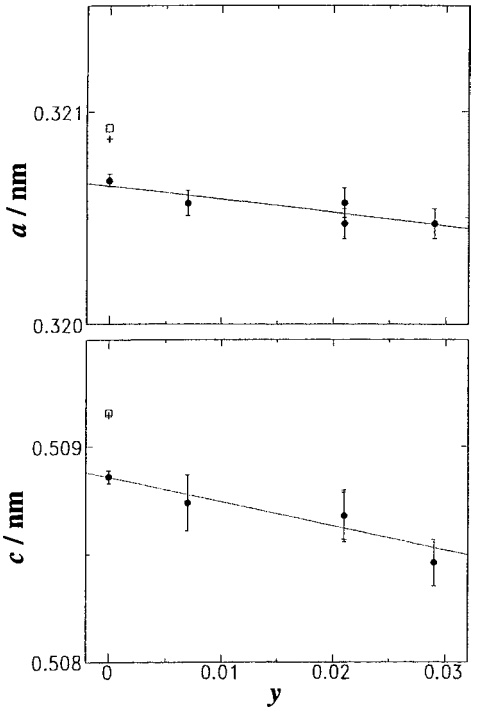

Fig. 2. Lattice parameters of *a*- and *c*-axes of $(Hf_{1-y}Al_y)O_{0.17}$ (y=0–0.03) at room temperature as a function of doped aluminium contents. (●) In this work. (+) By Dagerhamn [12]. (□) By Silver et al. [13].

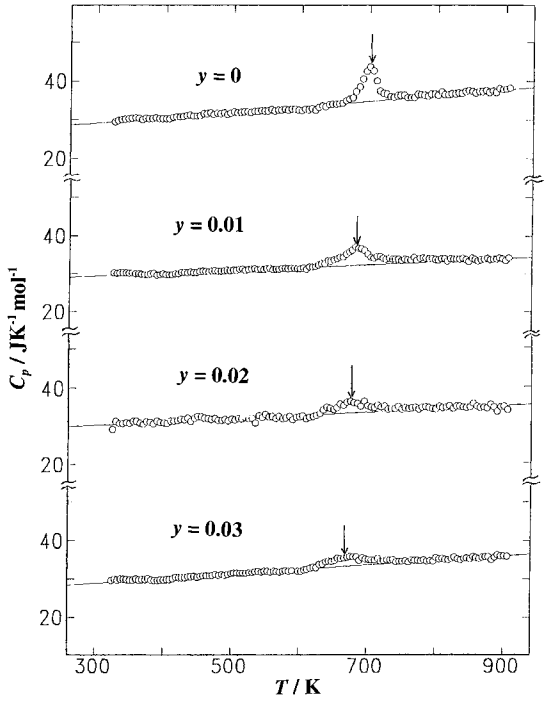

Fig. 3. Heat capacities of $(Hf_{1-y}Al_y)O_{0.17}$ (y=0–0.03) before annealing. The solid lines are the baselines determined by fitting heat capacity data excluding the heat capacity anomaly due to the order–disorder transition to a straight line. The arrows indicate transition temperatures.

3. Results and discussion

3.1. Lattice parameters of $(Hf_{1-y}Al_y)O_{0.17}$ samples

All the undoped and doped samples prepared were in a single phase having a hexagonal crystal structure. The *a* and *c* lattice parameters measured in this study are plotted as a function of doped aluminium contents in Fig. 2, where the results by Dagerhamn [12] and Silver et al. [13] are also shown. Both lattice parameters of the undoped samples determined in the present study are slightly smaller than those reported by the previous work [12,13]. The lattice parameters of $(Hf_{1-y}Al_y)O_{0.17}$ solid solutions decreased linearly with increasing aluminium contents, reflecting that hafnium atoms (r_{Hf}=144 pm) with a larger ionic radius are substituted for aluminium atoms (r_{Al}=125 pm) with a smaller ionic radius.

3.2. Heat capacity measurements of $(Hf_{1-y}Al_y)O_{0.17}$ samples

The results of the heat capacity measurements on $(Hf_{1-y}Al_y)O_{0.17}$ (y=0–0.03) before and after annealing are shown in Figs. 3 and 4, respectively. The heat capacity anomalies due to the order–disorder phase transitions occurred around 700 K for all the samples. However, the peak areas for the samples before annealing are much smaller than those for the well-annealed samples. It is likely that the unannealed sample had been only partially ordered. We refer the peaks at 700 K as the high temperature heat capacity anomaly in this paper.

Another anomalous effect occurred for the well-annealed samples in the lower temperature range up to 600 K. These anomalies did not occur for unannealed samples. We refer to it as the low temperature anomaly in this paper. Similar low temperature anomalies have been observed for undoped titanium–oxygen

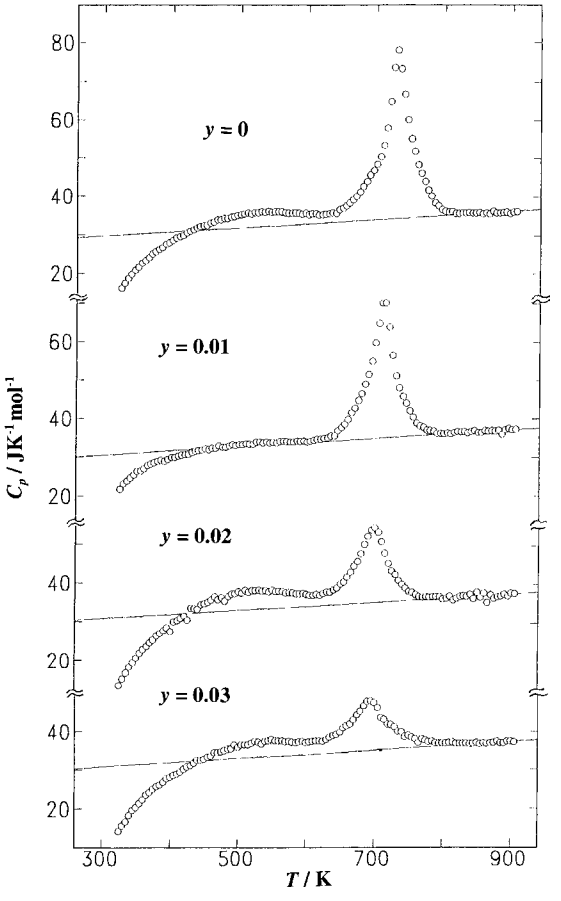

Fig. 4. Heat capacities of $(Hf_{1-y}Al_y)O_{0.17}$ (y=0–0.03) after annealing. The solid lines are the baselines of the heat capacity curves.

[6], zirconium–oxygen [7] and hafnium–oxygen [8,9] solid solutions.

3.2.1. Low temperature anomalous effect

We assumed that the low temperature anomaly was caused by poor heat conduction in a quartz vessel due to lowering helium gas pressure during annealing of the sample. In order to check this possibility, we performed a series of the following simple experiments in $ZrO_{0.24}$ sample in which similar low temperature anomaly was observed. At first, we measured the heat capacity on a sample resealed with helium gas pressure of 20 kPa after we confirmed existence of the low temperature anomaly for well-annealed sample as shown in Fig. 4. As expected, the low temperature anomaly disappeared and this heat capacity curve looked like heat capacity curves in Fig. 3. In next step, we measured heat capacity on a sample evacuated and sealed again in a quartz vessel. As a result, an anomaly similar to the low temperature anomaly appeared again. From these experimental facts, our assumption seems to be true. We could not examine the reason why helium gas pressure lowered during annealing. Considering that IVA transition metals have a property of dissolving a large amount of light elements, e.g., hydrogen, carbon, nitrogen and oxygen, some of helium may be absorbed in $(Hf_{1-y}Al_y)O_{0.17}$ during annealing.

3.2.2. Determination of the baseline of the heat capacity curve

In order to compute the experimental transition enthalpy and entropy changes of the order–disorder transition for the high temperature heat capacity anomaly, the baseline of the heat capacity curve has to be determined. However, it is difficult to determine the baseline by curve fitting heat capacity data, when there is a low temperature anomalous effect as seen in Fig. 4. We use the baseline of the unannealed samples which has no low temperature anomaly as seen in Fig. 3, as described in our previous study [8,9]. The baselines of the unannealed samples are determined by fitting the heat capacity data excluding the high temperature heat capacity anomaly to a straight line. These straight lines are shown as solid lines in Fig. 3. The slopes of these straight lines were found to be independent of the doped contents of the samples within the experimental error and also in good agreement with that of undoped hafnium metal without low temperature anomalous effect and high temperature heat capacity anomaly. Hence the average of these slopes was used as the slope of the baseline for the well-annealed samples having low temperature anomaly. The heat capacity data of well-annealed samples agreed well with those of unannealed ones above 830 K. The baseline of each sample was determined by minimizing the standard deviation of the heat capacity in the high temperature range above 830 K without heat capacity anomaly. In order to verify whether the method used here for the baseline determination was correct, the heat capacities of unannealed and well-annealed ZrO_x were measured. The baseline obtained by above mentioned method agreed with the baseline from the heat capacity analysis for

zirconium–oxygen alloys obtained in the previous work by the present author [7].

3.2.3. High temperature heat capacity anomaly

The enthalpy and entropy changes for the order–disorder transition of $(Hf_{1-y}Al_y)O_{0.17}$ samples which are not influenced by the low temperature anomalous effect were calculated on the basis of the baseline and the measured heat capacity data in Fig. 4. Typical example for the separation of the low and high temperature peaks is shown for $(Hf_{1-y}Al_y)O_{0.17}$ (y=0.02) sample in Fig. 5. The transition enthalpy is calculated by numerical integration of the shaded area in the figure, by assuming that the low temperature anomaly decreases linearly with increasing temperature after low temperature anomalous peak, as shown in the broken line in Fig. 5.

In order to check whether the transition enthalpy and entropy changes calculated by this method are correct, we performed two series of the following experiments for well-annealed $TiO_{0.22}$ sample in which similar low temperature anomaly was observed [14]. In the first run, we confirmed the existence of the low temperature anomalous effect and high temperature heat capacity anomaly for $TiO_{0.22}$ sample as shown in Fig. 5. The enthalpy and entropy changes in the first run were calculated by the same method described above. The sample was then loaded in the quartz vessel anew along with enough helium gas for heat conduction, and heat capacity measurement in the second run was carried out. As expected, the low temperature anomaly disappeared. The baseline in the first run is in good agreement with that in the second run. Transition enthalpy and entropy changes calculated from the excess heat capacity in the first run agree well with those in the second run within the experimental error [14].

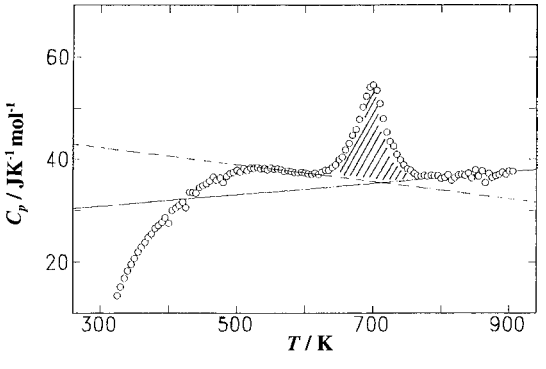

Fig. 5. Typical example for separation of low and high temperature heat capacity anomalies for y=0.02 sample. The solid line is the baseline of the heat capacity curves. The broken line is the decreasing line of the low temperature heat capacity anomaly.

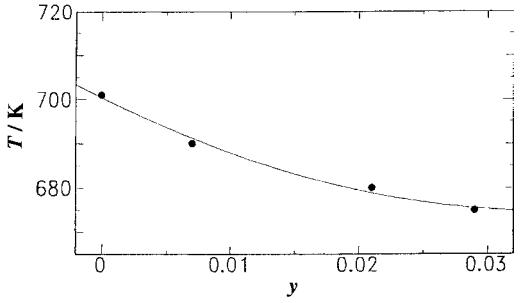

Fig. 6. Transition temperatures (T_t) of $(Hf_{1-y}Al_y)O_{0.17}$ (y=0–0.03) as a function of doped aluminium contents.

Figs. 6–8 show the transition temperatures, enthalpy change and entropy change due to the order–disorder transition obtained in this study, respectively, as a function of the doped aluminium contents. The temperature corresponding to the maximum heat capacity peak in Fig. 3 is regarded as the experimental transition temperature, because those peak temperatures before annealing shown in Fig. 3 are lower than those after annealing shown in Fig. 4 and are less affected by the time lag in heat conduction.

The theoretical transition entropy change for undoped HfO_x sample are calculated from configurational entropy change for the interstitial oxygen atoms in the host hafnium lattice between the ordered and disordered phases on the basis of crystal structure in Fig. 1b as described in our previous

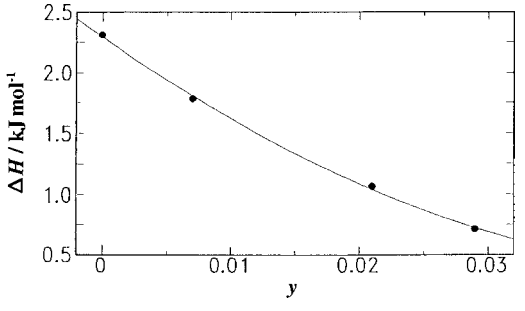

Fig. 7. Transition enthalpy changes (ΔH) of $(Hf_{1-y}Al_y)O_{0.17}$ (y=0–0.03) as a function of doped aluminium contents.

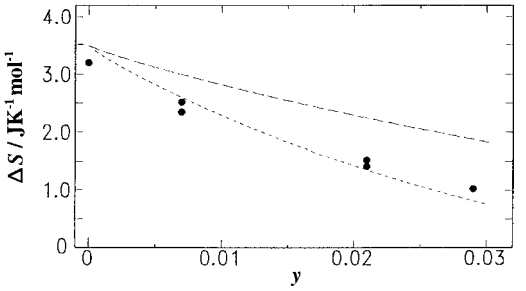

Fig. 8. Transition entropy changes (ΔS) of $(Hf_{1-y}Al_y)O_{0.17}$ (y=0–0.03) as a function of doped aluminium contents. (- - - - -) Theoretical entropy change calculated as p=l2 in Eq. (2). (– – –) Theoretical entropy change calculated as p=6 in Eq. (2).

paper [9]. The equation used for the calculation is as follows:

$$\Delta S = k \cdot [\ln\{{}_{N(1-x)}C_{Nx}\}] - k \cdot [\ln\{{}_{(N/6)}C_{N\{x-(1/6)\}} \cdot \alpha^{N\{x-(1/6)\}}\}], \quad (1)$$

where x, k and N are the O/Hf ratio, Boltzmann's constant and Avogadro's number, respectively. The factor 'α' is the number of the increasing configuration per one interstitial oxygen atom, comparing to the basic partially ordered phase as described below. On the right-hand side in Eq. (1), the first term is derived from the configurational entropy of the disordered phase. The second term of configuration ${}_{(N/6)}C_{N\{x-(1/6)\}}$ for the partially ordered state in Eq. (1) is derived by assuming that the excess interstitial oxygen atoms $N\{x-(1/6)\}$ occupy statistically the C sites (next inserted oxygen interstitial sites shown in Fig. 1) on the ideally ordered arrangement A□B□··· sequences in $HfO_{(1/6)(+)}$. The factor of α in the second term was determined to be α=17 from the composition (x) dependence of experimental transition entropy changes for $x\{\geqq\}$l/6 [9] As seen in Fig. 8, the theoretical transition entropy for $HfO_{1/6}$(∼$HfO_{0.17}$) sample calculated by using Eq. (1) is in good agreement with those obtained experimentally. This fact implies that the order–disorder transition for $HfO_{1/6}$ takes place from a complete ordered structure to disorder one which was proposed from crystal analyses in the electron and neutron diffraction experiments as reported by Hirabayashi et al. [10]. It has not been confirmed that titanium– and zirconium–oxygen solid solutions have been complete ordered structures for composition of x=1/6. Therefore, the existence of the complete ordered structure for $HfO_{1/6}$ may imply that the repulsive force between interstitial oxygen atoms in HfO_x is stronger than those in TiO_x or ZrO_x.

As also seen in Figs. 6–8, the transition temperatures, the enthalpies and entropies due to the order–disorder phase transition for $(Hf_{1-y}Al_y)O_{0.17}$ decreased with increasing aluminium contents. This may be explained by the fact that the insertion of the oxygen atoms into some of the interstitial sites is rejected by the substitution of smaller aluminium for hafnium host lattices and the numbers of the oxygen configuration are limited. By assuming α=17 and x=1/6 in Eq. (1), the theoretical transition entropy change for $(Hf_{1-y}Al_y)O_{1/6}$(∼$(Hf_{1-y}Al_y)O_{0.17}$) is expressed as follows:

$$\Delta S = k \cdot [\ln\{{}_{N\{1-(1/6)-yp\}}C_{(N/6)}\}] - k \cdot [\ln\{{}_{(1-yp)(N/6)}C_{(yp)(N/6)}\} \cdot \{17(1-yp)\}^{(yp)(N/6)}], \quad (2)$$

where p is the number of interstitial oxygen sites rejected by one doped aluminium atom. In Fig. 8, the theoretical transition entropies calculated as p=6 and p=12 in Eq. (2) are shown as the broken and dotted lines, respectively, as a function of the doped aluminium contents. As seen in Fig. 8, the value of p=12 is more suitable than that of p=6 in this study.

4. Conclusions

We measured heat capacities of $(Hf_{1-y}Al_y)O_{0.17}$ (y=0–0.03) from 325 to 905 K and obtained the following conclusions.

1. A heat capacity anomaly was observed around 700 K for well-annealed and unannealed $(Hf_{1-y}Al_y)$-$O_{0.17}$ samples and assigned to an order–disorder rearrangement of oxygen atoms. Anomalous effect at low temperature observed only for well-annealed samples may be caused by poor heat conduction in a quartz vessel due to lowering of helium gas pressure during annealing of the sample.
2. The experimental transition temperatures, the enthalpy changes and entropy changes due to the order–disorder phase transition for $(Hf_{1-y}Al_y)O_{0.17}$ decreased with increasing aluminium contents.

This may be explained by the fact that the insertion of the oxygen atoms into the interstitial site is disturbed by the substitution of smaller aluminium for hafnium host lattices and the numbers of the oxygen configuration are limited.

3. The experimental transition entropy change computed from heat capacity data for doped aluminium was in good agreement with the theoretical value calculated using a statistical thermodynamics.

References

[1] Wehlbeck et al., J. Am. Ceram. Soc. 49 (1966) 180.
[2] J.P. Abriata, J. Garces, R. Versaci, Bull. Alloy Phase Diagrams 7 (1986) 116.
[3] R.F. Domagala, R. Ruh, ASM Trans. Q. 58 (1965) 164.
[4] E. Rudy, P. Stecher, J. Less-Common Met. 5 (1963) 78.
[5] T. Tsuji, J. Nucl. Mater. 247 (1997) 63.
[6] T. Tsuji, M. Sato, K. Naito, Thermochim. Acta 163 (1990) 279.
[7] T. Tsuji, M. Amaya, K. Naito, J. Thermal Anal. 38 (1992) 1817.
[8] T. Kato, T. Tsuji, Thermochim. Acta 267 (1995) 397.
[9] T. Kato, T. Tsuji, J. Nucl. Mater. 247 (1997) 98.
[10] M. Hirabayashi, S. Yamaguchi, T. Arai, J. Phys. Soc. Jpn. 35 (1973) 473.
[11] T.B. Douglas, J. Natl. Bur. Standards. A 67 (1963) 403.
[12] T. Dagerhamn, Acta Chem. Scand. 15 (1961) 214.
[13] W.D. Silver, P.A. Farrar, K.L. Komarek, Trans. AIME 227 (1963) 876.
[14] Y. Nakamura, Master's Thesis of Graduate School of Engineering, Nagoya University, 1998.